Title
Modes of operation of the BKCa channel beta2 subunit.

Journal
The Journal of general physiology, 130(1)

ISSN
0022-1295

Authors
Savalli, Nicoletta
Kondratiev, Andrei
de Quintana, Sarah Buxton
et al.

Publication Date
2007-07-01

DOI
10.1085/jgp.200709803

Peer reviewed

Modes of Operation of the BK_{Ca} Channel β_2 Subunit

Nicoletta Savalli,[1] Andrei Kondratiev,[1] Sarah Buxton de Quintana,[1] Ligia Toro,[1,2,3,4] and Riccardo Olcese[1,3,4]

[1]Department of Anesthesiology-Division of Molecular Medicine, [2]Department of Molecular and Medical Pharmacology, [3]Brain Research Institute, and the [4]Cardiovascular Research Laboratory, David Geffen School of Medicine at University of California Los Angeles, Los Angeles, CA 90095

The β_2 subunit of the large conductance Ca^{2+}- and voltage-activated K^+ channel (BK_{Ca}) modulates a number of channel functions, such as the apparent Ca^{2+}/voltage sensitivity, pharmacological and kinetic properties of the channel. In addition, the N terminus of the β_2 subunit acts as an inactivating particle that produces a relatively fast inactivation of the ionic conductance. Applying voltage clamp fluorometry to fluorescently labeled human BK_{Ca} channels (hSlo), we have investigated the mechanisms of operation of the β_2 subunit. We found that the leftward shift on the voltage axis of channel activation curves (G(V)) produced by coexpression with β_2 subunits is associated with a shift in the same direction of the fluorescence vs. voltage curves (F(V)), which are reporting the voltage dependence of the main voltage-sensing region of hSlo (S4-transmembrane domain). In addition, we investigated the inactivating mechanism of the β_2 subunits by comparing its properties with the ones of the typical N-type inactivation process of *Shaker* channel. While fluorescence recordings from the inactivated *Shaker* channels revealed the immobilization of the S4 segments in the active conformation, we did not observe a similar feature in BK_{Ca} channels coexpressed with the β_2 subunit. The experimental observations are consistent with the view that the β_2 subunit of BK_{Ca} channels facilitates channel activation by changing the voltage sensor equilibrium and that the β_2-induced inactivation process does not follow a typical N-type mechanism.

The Journal of General Physiology

INTRODUCTION

The large conductance voltage- and Ca^{2+}-activated K^+ channels (BK_{Ca}) are widely distributed in cells and tissues (Salkoff et al., 2006), particularly in smooth muscles and in the central nervous system where their level of expression is significantly higher than in other tissues. In central neurons, BK_{Ca} channels control cell excitability and neurotransmitter release, coupling the membrane potential with intracellular Ca^{2+} levels (Gribkoff et al., 2001; Latorre and Brauchi, 2006). BK_{Ca} channels share many structural features with the family of voltage-gated K^+ channels with six membrane-spanning domains, such as the presence of the positively charged S4 segment that encodes for a functional voltage sensor (Stefani et al., 1997; Diaz et al., 1998), and the tetrameric association of four identical subunits (α) to form a functional channel (Shen et al., 1994). However, BK_{Ca} channels are unique in that they possess a seventh transmembrane domain (S0) that brings the N terminus extracellularly (Wallner et al., 1996) (Fig. 1 A) and a long intracellular C terminus domain that encodes for the Ca^{2+} sensitivity of the channel (Wei et al., 1994; Schreiber and Salkoff, 1997; Moss and Magleby, 2001; Xia et al., 2002; Zeng et al., 2005; Qian et al., 2006). Although only one gene (*hSlo*) encodes for the human BK_{Ca} channel (Wallner et al., 1995), the phenotypic variability of BK_{Ca} currents observed in different tissues is derived from alternative splice variants of the pore-forming α subunit (Zarei et al., 2001) and from the interaction with a variety of modulatory partners, such as the β subunits (Lu et al., 2006). In humans, four genes have been identified that encode for β subunits, reported as β_1, β_2, β_3, and β_4 (Tseng-Crank et al., 1996; Jiang et al., 1999; Wallner et al., 1999; Behrens et al., 2000; Brenner et al., 2000; Weiger et al., 2000). They share structural similarities: two transmembrane segments are connected by an extracellular loop and the N and C termini are intracellular (Fig. 1 A) (for review see Orio et al., 2002). Functional BK_{Ca} channels are thought to be formed by the association of four pore-forming α subunits and one to four accessory β subunits (Wang et al., 2002). The coexpression of α with β_1, β_2, and β_4 subunits modifies the apparent Ca^{2+}/voltage sensitivity, while all the β subunits alter the ionic current kinetics and the pharmacological properties of BK_{Ca} channels (Wallner et al., 1995, 1999; Hanner et al., 1997; Nimigean and Magleby, 1999; Behrens et al., 2000; Brenner et al., 2000; Meera et al., 2000; Xia et al., 2000; Lippiat et al., 2003; Ha et al., 2004; Wang et al., 2006). In addition, it has been recently shown that both the β_1 and the β_2 subunits can also modulate hSlo expression level through an endocytic mechanism

Correspondence to Riccardo Olcese: rolcese@ucla.edu

Abbreviations used in this paper: ANCOVA, analysis of covariance; COVG, cut-open oocyte technique; HP, holding potential; MES, methanesulfonate; TMRM, tetramethylrhodamine-5′-maleimide.

(Toro et al., 2006; Zarei et al., 2007). A recent work by Bao and Cox (2005) has demonstrated that the β_1 coexpression stabilizes the active state of the voltage sensor, consequently increasing the apparent Ca^{2+}/voltage sensitivity of the channel. A striking feature of the β_2 and isoforms of β_3 subunits is their ability to confer fast inactivating properties to the channel (Wallner et al., 1999; Xia et al., 1999, 2000; Uebele et al., 2000; Hu et al., 2003; Zeng et al., 2007). The NMR structure of the β_2 N terminus domain shows that this region consists of a helical core (residues 20–45, chain domain) and a flexible disordered motif (residues 1–18, ball domain) (Bentrop et al., 2001). The mechanism proposed is an N-type–like inactivation (i.e., "ball and chain" mechanism) in which 18 amino acids from the β_2 N terminus rapidly occludes the cytoplasmic mouth of the channels when they are in the open state (Wallner et al., 1999). The N-type inactivation mechanism described for fast inactivation in Na^+ and K^+ (*Shaker*) channels has been shown to be associated to the voltage sensor long-lasting permanence in its activated state, retarding its return to the resting position upon repolarization ("charge immobilization") (Armstrong and Bezanilla, 1977; Bezanilla and Armstrong, 1977; Bezanilla et al., 1991; Perozo et al., 1992; Roux et al., 1998).

Using the voltage clamp fluorometry technique (Mannuzzu et al., 1996) we have recently characterized the voltage-dependent conformational changes of the voltage-sensing region of hSlo channels during activation (Savalli et al., 2006). In this work, in order to gain insights on the mechanisms by which β_2 subunit facilitates channel opening and produces inactivation, we have studied the conformational changes occurring in BK_{Ca} voltage-sensing region in the presence of its β_2 modulatory subunits. We found that the β_2 subunit affects the movements and the equilibrium of the S3–S4 region, suggesting that the β_2 subunit promotes channel opening by favoring the activated conformation of the voltage-sensing region of BK_{Ca} channels. In addition, we have investigated whether the coexpression of the β_2 subunit affects the voltage sensor return to the resting position upon repolarization, i.e., induces "charge immobilization." We found no evidence of voltage sensor immobilization due to the docking of the β_2-inactivating particle into BK_{Ca} channel pore, suggesting an inactivating mechanism not homologous to the classically described N-type.

MATERIALS AND METHODS

Molecular Biology

We have used the α subunit of human BK_{Ca} (*hSlo*) (GeneBank/EMBL/DDBJ accession no. U11058), previously modified in a way that all native extracellular cysteines (C14S, C141S, and C277S) are substituted with serines and containing the R207Q mutation to increase open probability (Diaz et al., 1998). In hSlo cysteine-less R207Q background, a single cysteine was introduced at three positions in the S3–S4 linker (200, 201, and 202, see Fig. 1 B) by overlap mutagenesis PCR (Ho et al., 1989). The α subunit is cloned in the pBSTA vector, whereas the human β_2 subunit (GeneBank/EMBL/DDBJ accession no. AF099137) is in the pcDNA3 vector. The nonconducting *Shaker* K^+ channel mutant (Sh W434F) (Perozo et al., 1993) (GeneBank/EMBL/DDBJ accession no. M17211) and its inactivation-removed version (Sh-IR W434F) were also used. For site-directed fluorescent labeling of the S4 region with thiol-reactive fluorophores, we introduced a unique cysteine in the S3–S4 linker using the QuickChange site-directed mutagenesis kit (Stratagene), generating the Sh M356C W434F and Sh-IR M356C W434F mutants. All of the mutations were confirmed by sequence analysis. cRNAs were prepared in vitro (mMESSAGE mMACHINE; Ambion) and stored at −80°C.

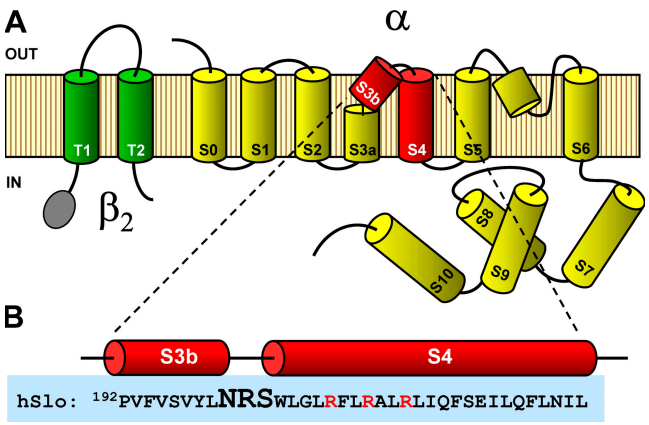

Figure 1. Schematic topology of BK_{Ca} α and β_2 subunits. (A) BK_{Ca} α subunit is formed by seven trasmembrane domains (S0–S6), an extracellular N terminus and a long intracellular C terminus, which comprises four hydrophobic domains (S7–S10). β_2 subunit possesses two transmembrane domains (T1 and T2) and an N-terminus that confers the inactivating properties to the channel. (B) Detail of the S3–S4 region illustrating the position of the three residues (NRS) that have been individually substituted with cysteines and labeled with different fluorophores (see Materials and Methods).

Expression and Labeling

Xenopus laevis (NASCO) oocytes (stage V-VI) were prepared as previously described (Haug et al., 2004), injected with 50 nl of total cRNA either of the mutant α subunits (0.01–0.1 μg/μl) alone or α+β_2 subunits (0.5–1 μg/μl) using a Drummond nanoinjector. Injected oocytes were maintained at 18°C in an amphibian saline solution supplemented with 50 μg/ml gentamycin (Invitrogen), 200 μM DTT, and 10 μM EDTA. 3–9 d after injection, oocytes were stained for 30–45 min with 10 μM membrane-impermeable thiol-reactive fluorescent dyes, tetramethylrhodamine-5′-maleimide (TMRM) or PyMPO-maleimide (Molecular Probes) in depolarizing K^+ solution (in mM: 120 K-methanesulfonate [MES], 2 Ca-MES, and 10 HEPES, pH 7). These fluorophores were dissolved in DMSO (100 mM stock concentration) and stored at −20°C. Changes in fluorescence emission were due to environmental differences sensed by the fluorophores.

Electrophysiology

Patch Clamp. Membrane patches of *Xenopus* oocytes in the inside-out configuration were perfused with bath solutions containing (in mM) 115 K-MES, 5 KCl, 5 HEDTA, 10 HEPES. The free $[Ca^{2+}]$ was varied by adding $CaCl_2$. The free $[Ca^{2+}]$ was first theoretically

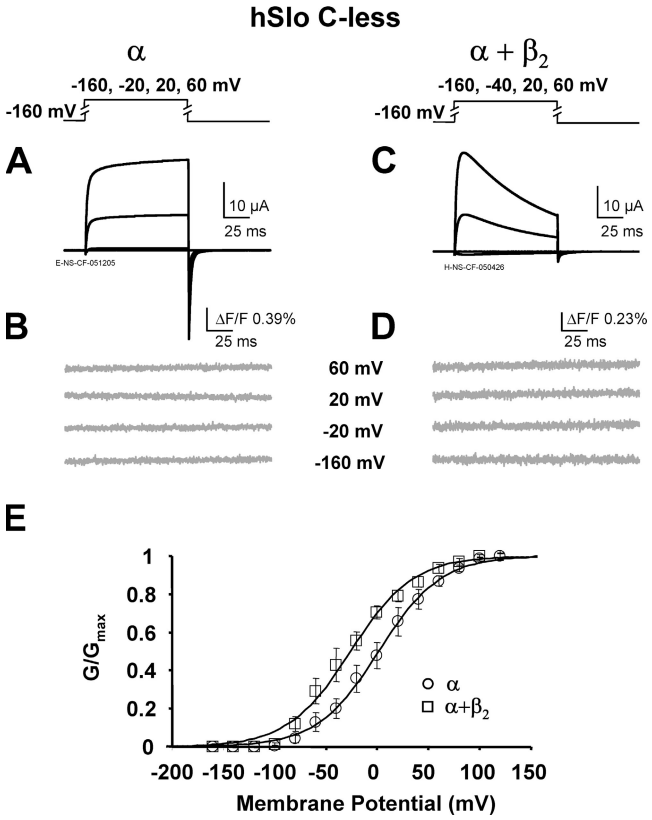

Figure 2. Lack of voltage-dependent fluorescence changes in the hSlo C-less background channel. Representative K^+ current traces from oocytes expressing α (A) and α+β_2 (C), elicited by 100-ms depolarization from −160 mV to the indicated potential. The corresponding TMRM fluorescence traces are shown in B and D. Holding potential (HP) was −90 mV. In C, the time-dependent decay of the ionic current is caused by the inactivating properties conferred to the BK_{Ca} channel by β_2 subunits. Note that no fluorescence changes (ΔF) were detected in hSlo C-less. (E) Averaged G(V) curves for α (○) and α+β_2(□) and the best fits to one Boltzmann distribution are shown superimposed (see Materials and Methods). Coexpression of the β_2 subunit produced ∼20 mV shift of the G(V) curve toward more negative potential (fitting parameters: α, V_{half} = 1.44 mV and z = 0.84; α+β_2, V_{half} = −26.13 mV and z = 0.83). Error bars represent SEM.

calculated with WEBMAXC v2.10 (http://www.stanford.edu/~cpatton/maxc.html) and then measured using a Ca^{2+} electrode (World Precision Instruments). Solutions were titrated to pH 7.0. The borosilicate pipettes (World Precision Instruments) were filled with the bath solution at lowest free [Ca^{2+}] (0.067 μM). The holding potential (HP) was –90 mV. All experiments were performed at 22–24°C. A prepulse to –160 mV (100 ms) or to –240 mV (25 ms) was delivered before the test pulse, as indicated in the figures.

Cut Open. Fluorescence, ionic, and gating currents were recorded in voltage clamp condition using the cut-open oocyte technique (COVG) (Stefani and Bezanilla, 1998) implemented for epifluorescence measurement (Cha and Bezanilla, 1998; Savalli et al., 2006). The extracellular solution contained (in mM) 60 Na-MES, 2 $Ca(MES)_2$, 10–50 K-MES, and 10 Na-HEPES (pH 7); whereas the intracellular solution contained (in mM) 110 K-glutamate and 10 K-HEPES (pH 7). The oocyte was impaled with a glass pipette filled with solution containing (in mM) 3,000 Na-MES, 10 NaCl, and 10 HEPES (pH 7). Gating currents were recorded unsubtracted, after analogue compensation of the membrane linear capacity and resistive components using a test pulse from 20 to 30 mV. The HP was –90 mV. All experiments were performed at 22–24°C.

Analysis

Experimental data were analyzed with a customized program developed in our Division and using fitting routines running in Microsoft Excel. The G(V) curves were calculated dividing the current/voltage relationships (IV curves) by the driving force (V_m-E_K), where V_m is the membrane potential and E_K the equilibrium potential for K^+, estimated using the Nernst equation. The IV curves for the α subunit expressed alone were constructed from the steady-state current at any given membrane potentials ranging from −240 to 240 mV (100-ms pulses). For the α+β2 subunit combination, because of the fast inactivation process, the IV curves were constructed from the peak current. Data for the membrane conductance (G(V)), the fluorescence (F(V)), and the gating charge (Q(V)) curves were fitted to one (hSlo) or two (*Shaker*) Boltzmann distributions of the form:

$$G(V) = \frac{G_{max}}{1 + e^{\left[z(Vhalf - Vm)\left(\frac{F}{RT}\right)\right]}};$$

$$F(V) = \frac{F_{max} - F_{min}}{1 + e^{\left[z(Vhalf - Vm)\left(\frac{F}{RT}\right)\right]}} - F_{min};$$

$$Q(V) = \frac{Q_{max} - Q_{min}}{1 + e^{\left[z(Vhalf - Vm)\left(\frac{F}{RT}\right)\right]}} - Q_{min},$$

where G_{max}, F_{max}, and Q_{max} are the maxima G, F, and Q; F_{min} and Q_{min} are the minima F and Q; z is the effective valence of the distribution; V_{half} is the half-activating potential; V_m is the membrane potential; and F, R, and T are the usual thermodynamic constants.

The analysis of covariance (ANCOVA) was performed to asses statistical significance of the change in V_{half} (for a range of log[Ca^{2+}]) induced by the coexpression of the β_2 subunit.

RESULTS

The Cysteine-less hSlo Coexpressed with the β_2 Subunit Does Not Elicit Voltage-dependent Fluorescence Changes

We have first evaluated the possibility that the cysteine-less hSlo clone (C-less) (used as a background construct in this study) expressed alone or together with the β_2 subunit could elicit voltage-dependent fluorescence signal after incubation with thiol-reactive fluorophores (TMRM and PyMPO). As shown in Fig. 2 A, under voltage clamp conditions, the expression of the C-less channel gave rise to a robust K^+ current elicited by membrane depolarizations. C-less channels constituted only by α subunits lacking all of the extracellularly exposed cysteines (C14S, C141S, and C277S) did not display any voltage-dependent change in TMRM fluorescence emission ΔF (the maximum ΔF/F = 0.0057% ± 0.0015%, n = 4) (Fig. 2 B). The coexpression of the C-less channels with the β_2 subunits produced a relatively fast inactivating current (Fig. 2 C) due to the docking of the β_2 N terminus

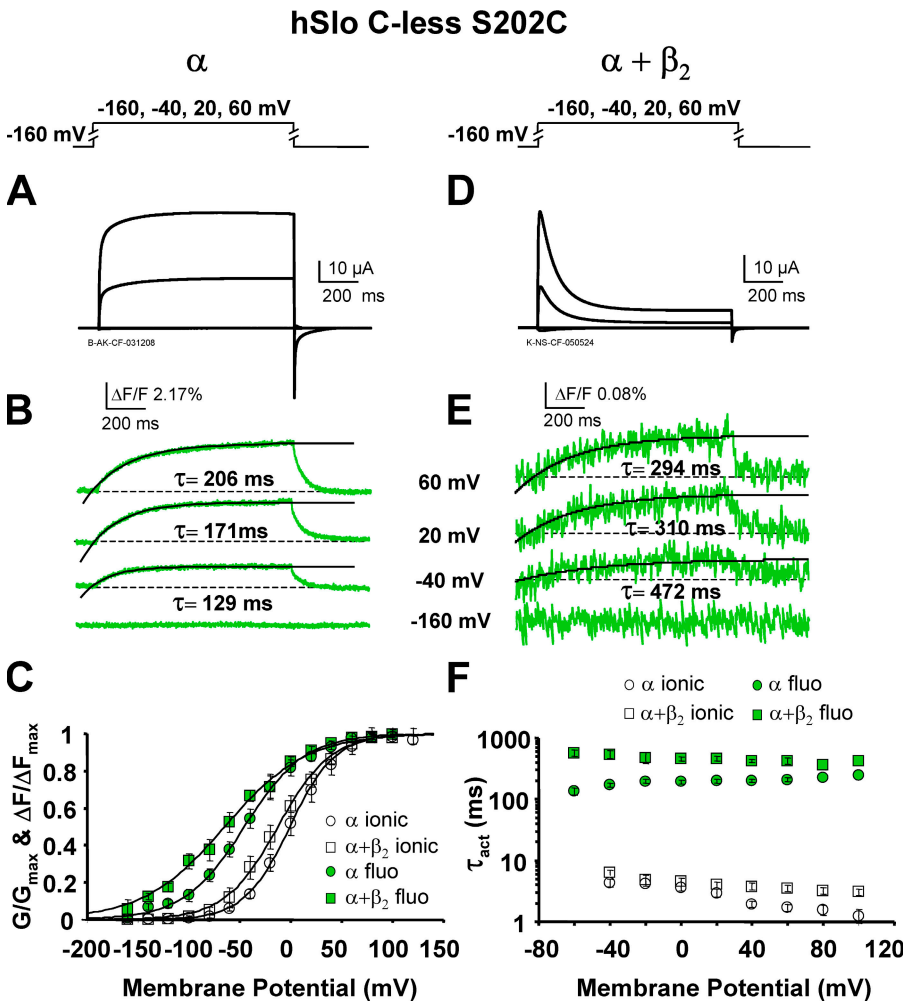

Figure 3. Conformational changes in α and α+β_2 reported by PyMPO at labeling position 202. Representative K^+ current traces from oocytes expressing α (A) and α+β_2 (D), elicited by 1-s depolarization from −160 mV to the indicated potential (HP = −90 mV). The corresponding fluorescence traces and the best fits to a single exponential function are shown superimposed in B and E. (C) Averaged F(V) and G(V) curves for α (G(V), ○, and F(V), ●) and α+β_2 (G(V), □, and F(V), ■). Data points are fitted to a single Boltzmann distribution and normalized to the respective maxima and minima (see Materials and Methods). Note that the coexpression of β_2 subunits produced a G(V) leftward shift of ∼15 mV associated to a corresponding shift of the F(V) (∼20 mV). G(V) fitting parameters are: α, V_{half} = 0.94 mV and z = 1.08; α+β_2, V_{half} = −13.02 mV and z = 1.00. F(V) fitting parameters are: α, V_{half} = −43.50 mV and z = 0.78; α+β_2, V_{half} = −68.69 mV and z = 0.62. (F) Kinetics of fluorescence and current activation. Both current and fluorescence activation were approximated to one exponential function. The coexpression of β_2 subunits reduced the rate of current activation in all potentials range (at 40 mV, τ_α = 2.52 ± 0.18 ms, n = 6, and $\tau_{\alpha+\beta2}$ = 3.89 ± 0.62 ms, n = 4). A similar effect of the β_2 subunits is observed on the rate of the fluorescence onset (at 40 mV, τ_α = 200 ± 13.24 ms, n = 6, and $\tau_{\alpha+\beta2}$ = 392.67 ± 19.83 ms, n = 4). Error bars represent SEM.

into the BK_{Ca} channel inner pore region. Also in this case, no voltage-dependent fluorescence changes were detected (the maximum ΔF/F = −0.0103% ± 0.002%, n = 3), suggesting that the eight endogenous cysteines present in the extracellular loop of β_2 (C84, C97, C101, C105, C113, C142, C148, and C178) are either not accessible by the fluorophore or do not report voltage-dependent rearrangements during depolarization and/or channel gating (Fig. 2 D). The normalized activation curves (G(V)) constructed from channels composed by only α (○) or α+β_2 (□) subunits labeled with TMRM are shown in Fig. 2 E. The coexpression of β_2 with C-less R207Q facilitated channel opening as shown by the parallel leftward shift of the G(V) curve on the voltage axis by ∼20 mV (α, V_{half} = −3.97 ± 10.15 mV, z = 0.91 ± 0.07, n = 4; and α+β_2,V_{half} = −25.91 ± 6.31 mV, z = 0.88 ± 0.04, n = 3). This effect of β_2 subunits is in general agreement with previous studies in WT hSlo and mSlo channels (Wallner et al., 1999; Xia et al., 1999). Similar results were obtained after incubation with a different fluorophore, PyMPO (Savalli et al., 2006; unpublished data).

The β_2 Subunit Affects the Kinetics and Voltage Dependence of both Ionic Current and Voltage Sensor Movements

Position 202. Based on the alignment with Shaker channel, Diaz et al. (1998) proposed that the outmost residue in BK_{Ca} S4 segment is W203. We first investigated the effect of β_2 on the conformational changes reported by PyMPO labeling S202C mutant. As shown in Fig. 3, the expression of S202C mutant gave rise to large ionic currents (A) associated to a rather slow voltage-dependent fluorescence change (ΔF) (B). The fluorescence vs. voltage curves (F(V)) (●) preceded the G(V) curves (○) on the voltage axis, as expected for conformational changes associated with the movement of the voltage sensor (Fig. 3 C). Coexpression with β_2 subunits affected several properties of both ionic current and fluorescence signal as follows. (a) The β_2 subunit induced a rapid inactivation to the ionic current as a consequence of the inactivating mechanism involving its N terminus (Fig. 3 D) (Wallner et al., 1999). (b) The G(V) curve for α+β_2 was shifted on the voltage axis toward a hyperpolarized direction by ∼15 mV and, surprisingly, also the voltage

TABLE I

Summary of Parameters Fitting G(V) and F(V) Curves to a Single Boltzmann Distribution

	S202C		R201C		N200C	
	G(V)	F(V)	G(V)	F(V)	G(V)	F(V)
$V_{half\ \alpha}$ (mV)	1.93 ± 6.57 (n = 5)	−44.30 ± 6.67 (n = 5)	15.40 ± 3.80 (n = 10)	−22.55 ± 3.58 (n = 10)	−12.68 ± 4.18 (n = 5)	−82.43 ± 3.03 (n = 5)
$V_{half\ \alpha+\beta2}$ (mV)	−11.71 ± 7.61 (n = 5)	−64.53 ± 4.87 (n = 5)	6.74 ± 2.27 (n = 8)	−57.19 ± 4.45 (n = 8)	−16.95 ± 5.13 (n = 3)	−101.0 ± 7.65 (n = 3)
z_α	1.15 ± 0.08 (n = 5)	0.83 ± 0.06 (n = 5)	1.05 ± 0.04 (n = 10)	0.80 ± 0.06 (n = 10)	0.90 ± 0.01 (n = 5)	0.91 ± 0.06 (n = 5)
$z_{\alpha+\beta2}$	1.06 ± 0.05 (n = 5)	0.63 ± 0.02 (n = 5)	1.04 ± 0.08 (n = 8)	0.72 ± 0.04 (n = 8)	1.0 ± 0.06 (n = 3)	0.72 ± 0.02 (n = 3)
$(\Delta F/F)/G_{max\ \alpha}$ (μS^{-1})	61.09 ± 13.13 (n = 5)		14.16 ± 2.46 (n = 10)		3.50 ± 1.14 (n = 5)	
$(\Delta F/F)/G_{max\ \alpha+\beta2}$ (μS^{-1})	27.62 ± 12.29 (n = 5)		9.96 ± 1.49 (n = 8)		3.73 ± 1.62 (n = 3)	

Data are reported as mean ± SEM.

dependence of fluorescence signal was negatively shifted by β_2 by ~20 mV in the same direction (Fig. 3 C; Table I). (c) The fluorescence signal was significantly attenuated by ~55% after coexpression with β_2 subunits: the ratio (for α alone) $(\Delta F_{max}/F)/G_{max} = 61.1 \pm 13.1\ \mu S^{-1}$ ($n = 5$) decreased to $27.6 \pm 12.3\ \mu S^{-1}$ ($n = 5$) in the presence of β_2 (Fig. 3 E), where $\Delta F_{max}/F$ is the maximum fluorescence change and G_{max} the limiting membrane conductance. (d) The kinetics of both ionic current activation (Meera et al., 1996; Brenner et al., 2000; Orio and Latorre, 2005) and fluorescence rising phase were significantly slowed down by the presence of the auxiliary subunit (Fig. 3 F). For example, at 40 mV, the time constants (τ) of ionic current activation (approximated to a single exponential function) were $\tau_\alpha = 1.91 \pm 0.18$ ms ($n = 6$) and $\tau_{\alpha+\beta2} = 3.89 \pm 0.62$ ms ($n = 4$) for α and $\alpha+\beta_2$, respectively. Similarly the time constants for the fluorescence onset of α and $\alpha+\beta_2$ (well fitted to a single exponential function) were $\tau_\alpha = 200.0 \pm 13.24$ ms ($n = 6$) and $\tau_{\alpha+\beta2} = 392.67 \pm 19.83$ ms ($n = 4$). In contrast, the effective gating charge (z) was not affected by β_2 (Table I), in agreement with recent findings (Orio and Latorre, 2005).

These experimental evidences suggest that the β_2 subunit facilitates voltage sensor activation by altering its equilibrium such that BK_{Ca} channel can reach higher open probability for the same membrane depolarization.

Position 201. In hSlo channel, the extracellular linker between S3 and S4 transmembrane segments is probably formed by no more than three residues (N200-R201-S202) (Diaz et al., 1998; Wallner et al., 1999; Ma and Horrigan, 2005). All these residues can report voltage-dependent conformational changes related to the movement of the main BK_{Ca} voltage sensor (Savalli et al., 2006). We speculate that the β_2 effects observed on S202C construct should be similar to the ones reported by the other two positions in the S3–S4 linker. To test this hypothesis, we labeled R201C with PyMPO and simultaneously recorded the ionic current and the fluorescence signals from oocytes expressing the pore-forming α subunit alone (Fig. 4, A and B) or together with β_2 subunits (Fig. 4, C and D). The onset of the fluorescence signal during depolarization was faster in R201C than in S202C, thus 100-ms pulses were adequate to reach steady state in this clone (Fig. 4, B and D, vs. Fig. 3, B and E). Similar to that observed for the adjacent position 202, PyMPO fluorescence reported by position 201 was reduced by ~30% when β_2 was coexpressed (Table I). Also in this mutant, the presence of β_2 subunit produced a parallel leftward shift of both current activation and fluorescence curves, as shown in Fig. 4 E. The midpoint of the F(V) was $FV_{half} = -22.55 \pm 3.58$ mV ($n = 10$) for α alone (●) and $FV_{half} = -57.19 \pm 4.45$ mV ($n = 8$) for $\alpha+\beta_2$ (■) (Fig. 4 E; Table I). As for S202C construct, the slowing of the ionic current activation kinetics induced by the auxiliary subunit was accompanied by a similar (but more pronounced) slowing of the fluorescence onset (Fig. 4 F). For depolarizations to 40 mV, the time constants of ionic current activation approximated to a single exponential function were $\tau_\alpha = 2.73 \pm 0.18$ ms ($n = 8$) and $\tau_{\alpha+\beta2} = 5.22 \pm 1.05$ ms ($n = 6$) for α and $\alpha+\beta_2$, respectively. The time constants for the fluorescence onset of α and $\alpha+\beta_2$ were $\tau_\alpha = 3.47 \pm 0.09$ ms ($n = 8$) and $\tau_{\alpha+\beta2} = 17.35 \pm 3.69$ ms ($n = 6$).

Position 200. As reported previously (Savalli et al., 2006), position 200 did not elicit significant voltage- dependent ΔF when labeled with PyMPO. Therefore, we investigated the conformational changes involving N200C construct using TMRM. Ionic current and fluorescence recordings from oocytes expressing α alone (Fig. 5, A and B) or $\alpha+\beta_2$ (Fig. 5, C and D) show that, in this mutant, the coexpression of β_2 subunit produced a relatively smaller shift of the channel activation curve toward hyperpolarized potentials (~5 mV). Nevertheless, this change in voltage dependence was associated to a well-resolved shift of the F(V) curve by ~20 mV in the same direction (Fig. 5 E; Table I). As for the other positions,

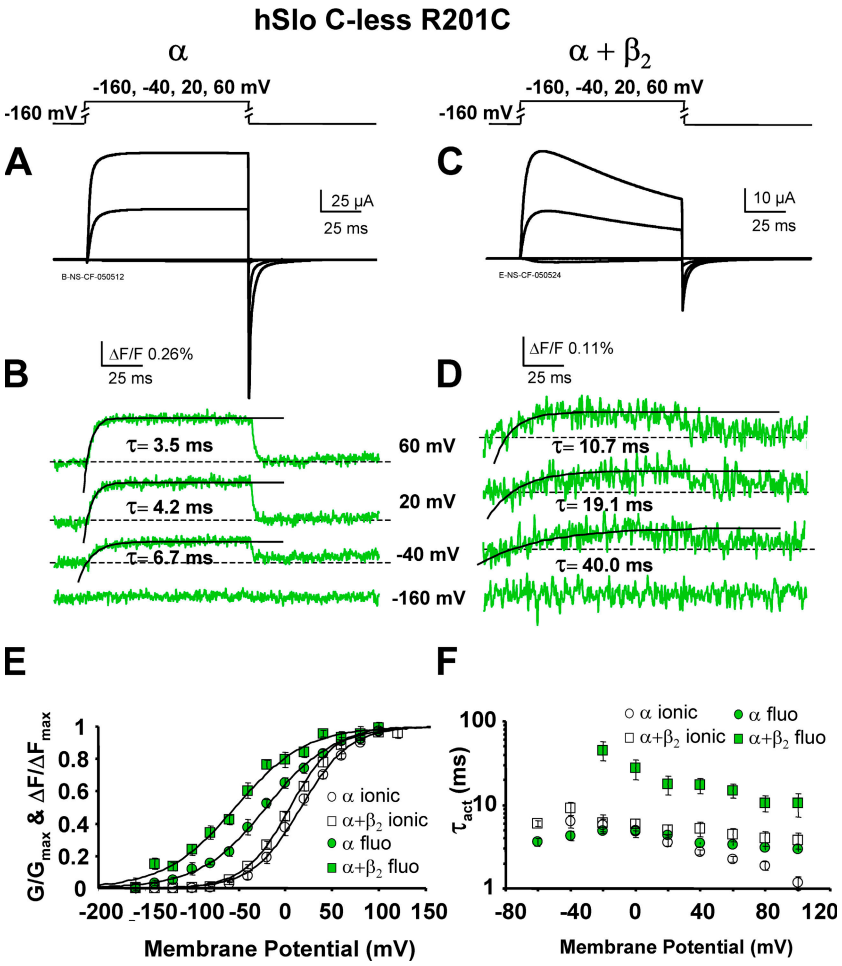

Figure 4. Conformational changes in α and $\alpha+\beta_2$ reported by PyMPO at labeling position 201. Representative K^+ current traces from oocytes expressing α (A) and $\alpha+\beta_2$ (C), elicited by 100-ms depolarization from −160 mV to the indicated potential (HP = −90 mV). The corresponding fluorescence traces and the best fits to a single exponential function are shown superimposed in B and D. (E) Averaged F(V) and G(V) curves for α (G(V), ○, and F(V), ●) and $\alpha+\beta_2$ (G(V), □, and F(V), ■). Data points are fitted to a single Boltzmann distribution and normalized to the respective maxima and minima (see Materials and Methods). Note that coexpression of β_2 subunits produced a leftward shift of the conductance curve (∼10 mV) associated to a corresponding more relevant shift of the fluorescence curve (∼30 mV). G(V) fitting parameters are: α, V_{half} = 16.73 mV and z = 0.98; $\alpha+\beta_2$, V_{half} = 3.72 mV and z = 1.06. F(V) fitting parameters are: α, V_{half} = −19.81 mV and z = 0.67; $\alpha+\beta_2$, V_{half} = −56.89 mV and z = 0.64. (F) Kinetics of fluorescence and current activation. Both current and fluorescence activation were approximated to one exponential function. The coexpression of β_2 subunits reduced the rate of current activation in all potentials range (at 40 mV, τ_α = 2.73 ± 0.18 ms, n = 8, and $\tau_{\alpha+\beta2}$ = 5.22 ± 1.05 ms, n = 6). A similar effect of the β_2 subunits is observed on the rate of the fluorescence onset (at 40 mV, τ_α = 3.47 ± 0.09 ms, n = 8, and $\tau_{\alpha+\beta2}$ = 17.35 ± 3.69 ms, n = 6). Error bars represent SEM.

ionic current activation kinetics was slowed down by the presence of β_2 subunit (at 40 mV, τ_α = 1.99 ± 0.30 ms, n = 5, and $\tau_{\alpha+\beta2}$ = 4.19 ± 0.45 ms, n = 3). Similarly, the time constant of the fluorescence onset slightly increased in the presence of β_2 subunit (at 40 mV, τ_α = 20.00 ± 3.80 ms, n = 5, and $\tau_{\alpha+\beta2}$ = 25.06 ± 3.06 ms, n = 3) (Fig. 5 F).

In summary, for all the positions tested, we have consistently observed a left shift in the activation curve, associated with a shift of the fluorescence vs. voltage curve in the same direction, when the modulatory β_2 subunit was coexpressed with the pore-forming α subunit. The G(V) shift observed is rather small, raising the question whether the oocyte internal $[Ca^{2+}]$ is low (in the submicromolar range) or the effect of β_2 subunit on the R207Q mutant is somewhat quantitatively different from the WT. We have addressed this point in the next section.

Ca^{2+} Dependence of the hSlo C-less R207Q S202C Mutant: Effect of the β_2 Subunit

The β_2 subunit facilitates WT BK_{Ca} channels opening in a wide range of Ca^{2+} concentrations. However, in the submicromolar range, the β_2 effect on the half activation potential is limited (Wallner et al., 1999; Orio and Latorre, 2005). Thus, a very low oocyte internal Ca^{2+} concentration could be the reason for the relatively small shift of the G(V) curves in the presence of the β_2 subunit observed in the COVG experiments.

To estimate the free intracellular Ca^{2+} concentration ($[Ca^{2+}]_i$) in the COVG experiments, we have characterized the Ca^{2+} dependence of the half activation potential (V_{half}) of the hSlo C-less R207Q S202C coexpressed with and without the β_2 subunit in *Xenopus* oocytes. Excised membrane patches in the inside-out configuration were perfused with solutions containing different free $[Ca^{2+}]_i$ ranging from 0.067 to 138 μM. K^+ currents were recorded during depolarizations ranging from −240 to 240 mV (Fig. 6, A–D). In average, the coexpression of the β_2 subunit facilitated channel opening as shown by the plot in Fig. 6 E reporting the V_{half} vs. free $[Ca^{2+}]_i$ for all the experiments. The lowering of the V_{half} induced by the β_2 subunit is significant ($P < 0.0001$) as revealed by the analysis of covariance (ANCOVA) adjusted for the log$[Ca^{2+}]$. The difference in V_{half} for $[Ca^{2+}]$ = 1 μM was −22.3 mV. These results are qualitatively in agreement with that previously reported for the WT channel coexpressed with the noninactivating β_2 mutant (β_2IR, inactivation removed), although the overall effect of the β_2 subunit on the activation of this mutant appears significantly smaller.

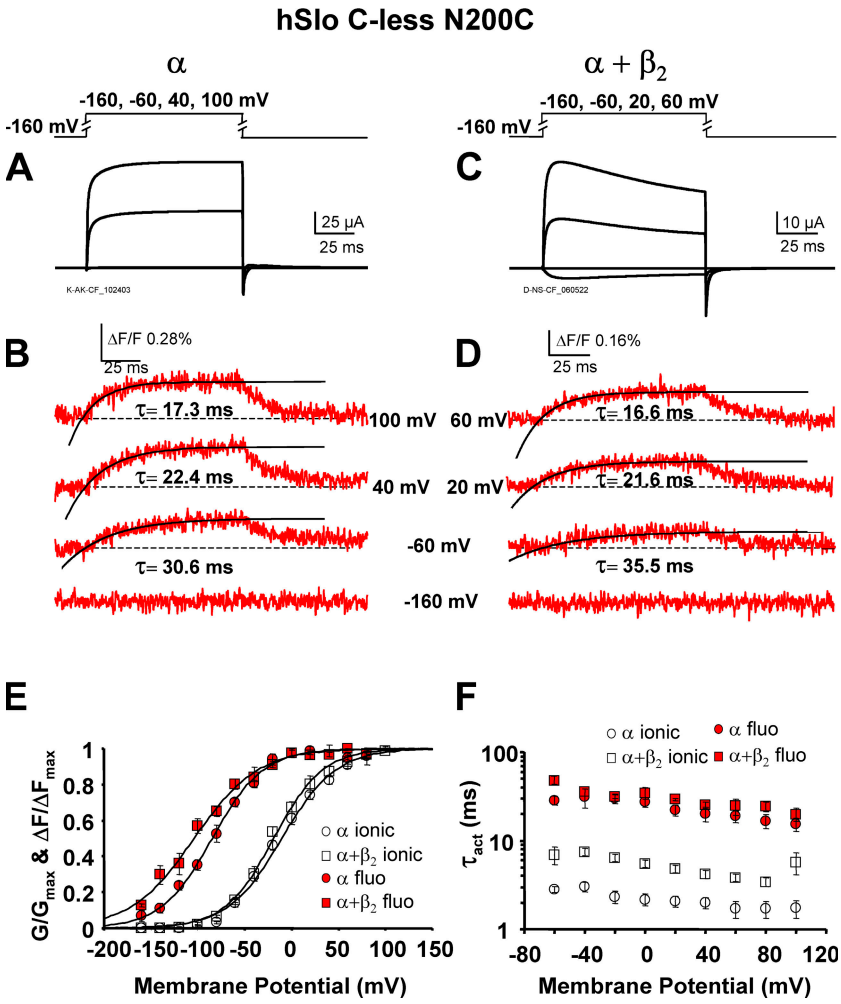

Figure 5. Conformational changes in α and $\alpha+\beta_2$ reported by TMRM at labeling position 200. Representative K^+ current traces from oocytes expressing α (A) and $\alpha+\beta_2$ (C), elicited by 100-ms depolarization from −160 mV to the indicated potential (HP = −90 mV). The corresponding fluorescence traces and the best fits to a single exponential function are shown superimposed in B and D. (E) Averaged F(V) and G(V) curves for α (G(V), ○, and F(V), ●) and $\alpha+\beta_2$ (G(V), □, and F(V), ■). Data points are fitted to a single Boltzmann distribution and normalized to the respective maxima and minima (see Materials and Methods). Note that coexpression of β_2 subunits produced a leftward shift of the conductance curve (∼5 mV) associated to a corresponding more relevant shift of the fluorescence curve (∼20 mV). G(V) fitting parameters are: α, V_{half} = −10.31 mV and z = 0.88; $\alpha+\beta_2$, V_{half} = −18.93 mV and z = 0.97. F(V) fitting parameters are: α, V_{half} = −84.57 mV and z = 0.93; $\alpha+\beta_2$, V_{half} = −103.66 mV and z = 0.75. (F) Kinetics of fluorescence and current activation. Both current and fluorescence activation were approximated to one exponential function. The coexpression of β_2 subunits reduced the rate of current activation at all potentials tested (at 40 mV, τ_α = 2.00 ± 0.28 ms, n = 5, and $\tau_{\alpha+\beta2}$ = 4.19 ± 0.45 ms, n = 3). Error bars represent SEM.

From the V_{half} vs. $[Ca^{2+}]_i$ plot, we estimated the free $[Ca^{2+}]_i$ of the COVG experiments. By rough interpolation, we calculated that the $[Ca^{2+}]_i$ is 3–4 μM. This value is in excellent agreement with the contaminant $[Ca^{2+}]_i$ of the internal solution (120 mM K-glutamate) measured with a Ca^{2+}-sensitive electrode (4.9 μM contaminant $[Ca^{2+}]_i$). Note that the K-glutamate solution faces the saponine-permeabilized oocyte membrane.

Thus, the effect of the β_2 subunit observed in the fluorescence experiments using the COVG technique (5–15 mV G(V) shift toward hyperpolarized potentials) is consistent with the results from the excised patch.

A Typical N-type Mechanism for β_2?

The N-type mechanism of channel inactivation has been well characterized and shown to directly affect the charge movement in Na^+ (Armstrong and Bezanilla, 1977) and in K^+ (*Shaker*) channels (Bezanilla et al., 1991; Perozo et al., 1992; Roux et al., 1998). Upon depolarization and channel opening, the inactivation particle binds to its docking site in the inner mouth of the pore, slowing the return of the voltage sensor to the resting conformation, thus preventing the channel deactivation. The electrical manifestation of this process is the so-called "OFF charge immobilization," since gating charge cannot return readily at the end of the depolarizing pulse, until the inactivating particle has been released from the inner pore. Since large part of the charge movement is produced by the translocation of the charged residues of the S4 segment, the effect of charge immobilization is indeed a partial immobilization of the S4 segment itself. To learn about the mechanism of inactivation in BK_{Ca} channel, we have investigated whether the β_2 subunit produces immobilization of the BK_{Ca} voltage sensor by directly assessing the movement of the S4 segment using an optical approach. As a reference, we have first characterized the immobilization of the voltage-sensing region in *Shaker* K^+ channel, a classical model for N-type inactivation (Hoshi et al., 1990; Bezanilla et al., 1991; Hoshi et al., 1991; Roux et al., 1998).

Optical Detection of *Shaker* S4 Segment Immobilization After N-type Inactivation

In the nonconducting (W434F) *Shaker* mutant (Perozo et al., 1993) we have fluorescently labeled position 356 in the S3–S4 linker using TMRM to track the movement

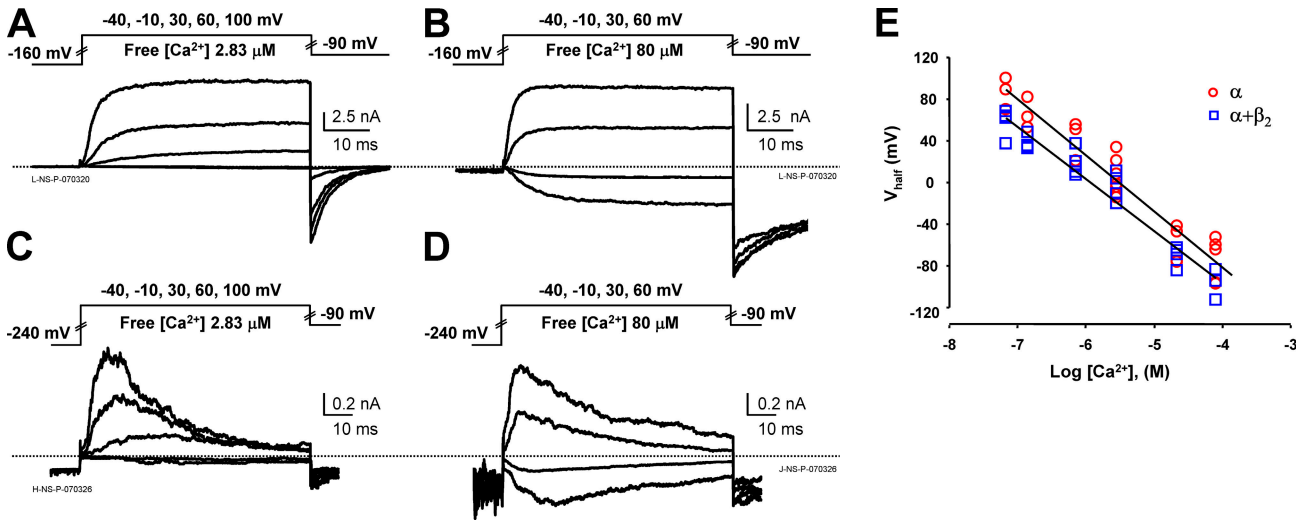

Figure 6. Ca^{2+} dependence of the half activation potential (V_{half}) in hSlo C-less R207Q S202C. (A and B) Representative K^+ current traces (unsubtracted) from excised patches of oocytes expressing hSlo α subunit elicited by 50-ms depolarizations from −160 mV to the indicated potential (HP = −90 mV). (C and D) Representative K^+ current traces from excised patches of oocytes expressing hSlo α+β_2 subunits elicited by 80-ms depolarizations from −240 mV to the indicated potential (HP = −90 mV). A 25-ms prepulse to −240 mV was necessary to recover channel from inactivation. (E) Scatter plot showing the dependence of V_{half} on the log[Ca^{2+}] for α (○) and α+β_2 (□). Continuous lines are the linear regression of the experimental data, shown superimposed. The β_2 subunit facilitates channel opening, significantly lowering the V_{half} in the range of [Ca^{2+}] tested ($P < 0.0001$) (ANCOVA).

of the main voltage-sensing region (Mannuzzu et al., 1996; Cha and Bezanilla, 1997). In Fig. 7 (A and B), we show families of gating currents recorded from *Shaker* channel having the N terminus deletion Δ6–46 that lacks N-type inactivation, Sh-IR M356C W434F (A), and from channels with intact N terminus, Sh M356C W434F (B). While, for all potentials tested, the ON gating currents are practically identical in the two clones, the OFF gating currents following voltage steps leading to channel opening (e.g., >−40 mV) display an extremely slow component reflecting a "charge immobilization" due to the inactivating N terminus (Fig. 7 B). On the other hand, in the mutant lacking the N-terminal inactivating domain, the OFF charge returns with a faster kinetics (i.e., it does not display charge immobilization) (Fig. 7 A). The corresponding fluorescence recordings that report the conformational changes of the voltage-sensing region for the two *Shaker* mutants are shown in Fig. 7 (C and D).

The steady-state properties of both charge and fluorescence changes are summarized in Fig. 8 A for the two *Shaker* mutants. The presence of the inactivating N terminus does not seem to affect the voltage dependence of the charge movement (Q(V)) or of the F(V) curves (Fig. 8 A).

The onset of the fluorescence change is practically identical in the two mutants in the range of potentials explored (from −60 to 20 mV) (Fig. 8 B). For example, at 10 mV the ON fluorescence time constants for inactivating (Sh) and noninactivating (Sh-IR) *Shaker* channels were τ_{Sh} = 6.18 ± 0.42 ms and $\tau_{Sh\text{-}IR}$ = 6.90 ± 0.53 ms (n = 5). On the contrary, the OFF fluorescence reveals dramatic differences in the kinetic behavior of the two channels (Fig. 8 C). In the Sh-IR channels, during repolarization to −90 mV after pulsing to 10 mV, the fluorescence follows a monoexponential decay, with a rather fast time course (τ = 3.44 ± 0.38 ms at 10 mV, n = 5) (Fig. 7 C and Fig. 8 C). On the other hand, in the channel with the intact N terminus, TMRM fluorescence reports the progressive S4 immobilization that becomes more prominent with larger depolarizations (Fig. 7 D). This is revealed by the appearance of a second slow component in the fluorescence relaxation that is absent in Sh-IR (during repolarization to −90 mV after pulsing to 10 mV, τ_{fast} = 2.74 ± 0.25 ms and τ_{slow} = 32.71 ± 0.20 ms, Amp_{fast} = 22.9% ± 2.9% and Amp_{slow} = 77.1% ± 2.9% at 10 mV, n = 5) (Fig. 8, C and D).

In conclusion, the fluorescent labeling of *Shaker* channel directly demonstrates the immobilization of the S4 segment, as a consequence of N-type inactivation.

The Inactivating Process of BK_{Ca} β_2 Subunit Does Not Involve the S4 Segment Immobilization in its Active State

We have applied to hSlo the same fluorescence-based strategy used for detecting S4 immobilization in *Shaker*. In BK_{Ca} channels labeled with PyMPO at position 202, we have compared the OFF fluorescence kinetics in the absence and in the presence of the inactivating β_2 subunit. As shown in Fig. 9 (B and D), the OFF fluorescence kinetics of the α subunit alone, during repolarization to −160 mV, is slightly faster than the one in the presence of the β_2 subunit, as expected, since the auxiliary

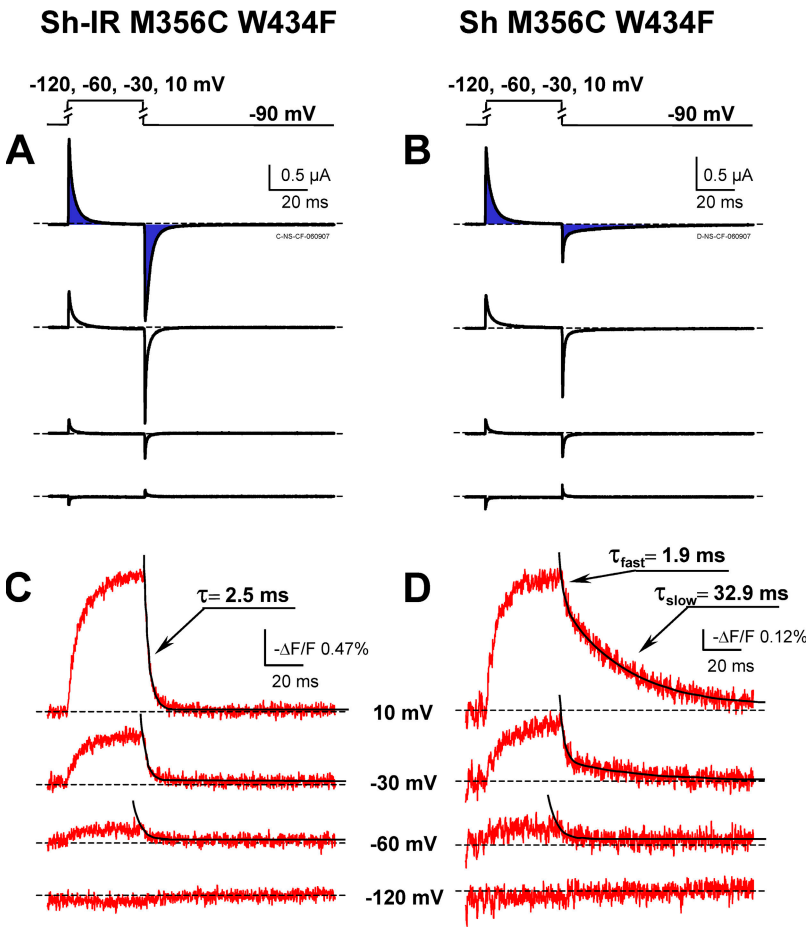

Figure 7. S4 immobilization revealed by OFF fluorescence kinetics in *Shaker* M356C W434F. Representative gating current traces from oocytes expressing Sh-IR M356C W434F (A) or Sh M356C W434F (B) elicited by 40-ms depolarization from −90 mV to the indicated potential (HP = −90 mV). Note the slow OFF-charge return in the presence of the intact N terminus (B). The corresponding fluorescence traces and the best fits to one (C) or two (D) exponential function(s) are shown superimposed in B and D. The appearance of a second component in the exponential function fitting fluorescence deactivation reveals the immobilization of the S4 segment in the activated position (at 10 mV, for Sh-IR $\tau = 3.44 \pm 0.38$ ms, $n = 5$, and for Sh $\tau_{fast} = 2.74 \pm 0.25$ ms and $\tau_{slow} = 32.71 \pm 0.20$ ms, $n = 5$).

subunit slows down the kinetics of both activation and deactivation of the channel (Meera et al., 1996; Brenner et al., 2000; Orio and Latorre, 2005). For example, after 1-s depolarization to 80 mV the OFF fluorescence time constants measured at −160 mV were $\tau_{\alpha} = 40.22 \pm 3.69$ ms ($n = 3$) (●) and $\tau_{\alpha+\beta2} = 51.31 \pm 2.51$ ms ($n = 3$) (■) (Fig. 9 I). However, the coexpression of the β_2 subunit does not cause the appearance of a second slower component in the fluorescence return, as found for *Shaker* channel, supporting the view that β_2-inactivating ball domain does not interfere with the voltage sensor deactivation. We obtained similar results for repolarization to −90 mV (Fig. 9, F, H, and I), where $\tau_{\alpha} = 78.93 \pm 2.29$ ms ($n = 3$) (●) and $\tau_{\alpha+\beta2} = 92.46 \pm 2.30$ ms ($n = 3$) (■). Note that the OFF fluorescence during repolarization to −90 mV does not return to baseline (−160 mV), due to the significant ΔF present between −160 and −90 mV, which is larger in $\alpha+\beta_2$ than in α alone (see F(V) curves in Fig. 3 C). Since it is possible that the OFF rate of the inactivating β_2 N-terminal "ball peptide" during repolarization is faster than the return of the voltage-sensing region, we have used a double pulse protocol to estimate the time course of the recovery from inactivation at different membrane potentials: −160, 120, and −90 mV (Fig. 10, A–E). We found that at −160 mV, 90% of the channels recovered from inactivation with a time constant of $\tau = 5.24 \pm 0.35$ ms ($n = 4$; Fig. 10 A). This time constant is ∼10 times faster than the one describing the OFF fluorescence kinetics, suggesting that at −160 mV, when the S4 segments are returning to their resting position, all the channels have already recovered from inactivation.

On the other hand, the recovery of the channel conductance from inactivation at −90 mV is biexponential with fast and slow component equally represented: $\tau_{fast} = 43.47 \pm 3.99$ ms (55%), $\tau_{slow} = 248.91 \pm 0.23$ ms (45%) ($n = 4$) (Fig. 10, F and G). Nevertheless, at −90 mV the OFF fluorescence relaxes with a time constant of $\tau = 92.46 \pm 2.30$ ms (Fig. 9 H), significantly faster than the overall recovery from inactivation at this potential. Thus, at −90 mV, the S4 segments appear to return to their resting position, while most of the channels are still inactivated. These results strongly suggest that the docking of the β_2 inactivating "ball" into the inner pore does not immobilize the BK_{Ca} voltage sensor in the active position, opposite to that observed in *Shaker* channel. In this aspect, BK_{Ca} channels do not follow a classically described N-type inactivation mechanism.

The lack of influence of the β_2 inactivation on the S3–S4 region conformational changes is also supported

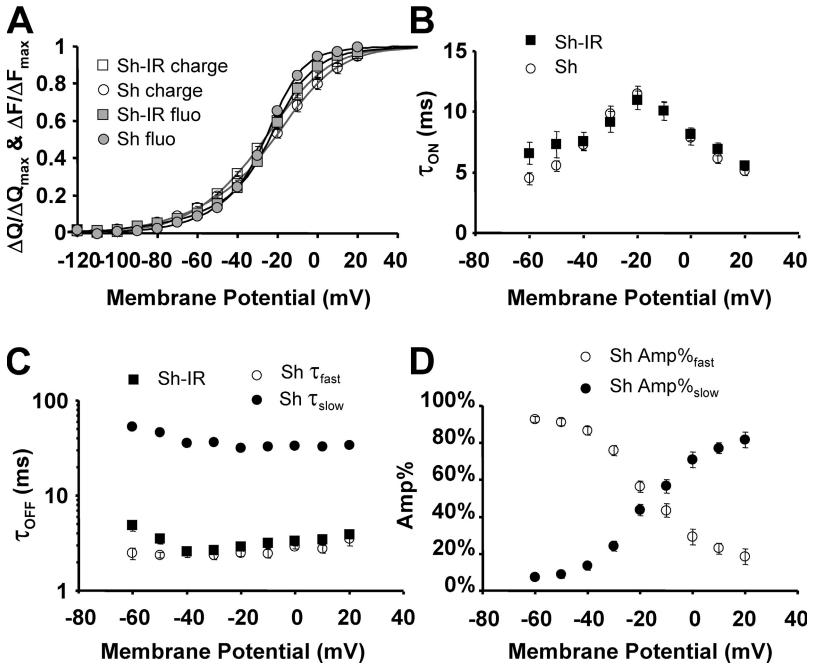

Figure 8. Evidences of S4 immobilization in *Shaker* channel from voltage clamp fluorometry. (A) Averaged Q(V) and F(V) curves for Sh (Q(V), ○, and F(V), ●) and Sh-IR (Q(V), □, and F(V), ■). Data points are fitted to two Boltzmann distributions and normalized to the respective maxima and minima (see Materials and Methods). Note that the inactivation process is not affecting the voltage dependence of both charge and fluorescence. The averaged parameters are as follows: in Sh-IR, for the Q(V) $V_{half}1 = -56.40 \pm 1.58$ mV, $z1 = 1.68 \pm 0.06$, $Q1 = 22.50 \pm 1.59\%$, $V_{half}2 = -21.01 \pm 1.31$ mV, $z2 = 1.86 \pm 0.05$, $Q2 = 77.50 \pm 1.59\%$ and for the F(V) $V_{half}1 = -44.53 \pm 1.93$ mV, $z1 = 1.17 \pm 0.08$, $F1 = 30.37 \pm 2.62\%$, $V_{half}2 = -20.38 \pm 1.50$ mV, $z2 = 2.79 \pm 0.19$, $F2 = 69.63 \pm 2.62\%$ $-\Delta F/F = 2.72 \pm 0.59\%$ ($n = 5$); in Sh, for the Q(V) $V_{half}1 = -61.72 \pm 2.04$ mV, $z1 = 1.50 \pm 0.17$, $Q1 = 18.44 \pm 2.26\%$, $V_{half}2 = -16.11 \pm 1.87$ mV, $z2 = 1.78 \pm 0.15$, $Q2 = 81.56 \pm 2.26\%$ and for the F(V) $V_{half}1 = -41.38 \pm 2.24$ mV, $z1 = 1.66 \pm 0.18$, $F1 = 34.30 \pm 3.44\%$, $V_{half}2 = -22.34 \pm 0.55$ mV, $z2 = 3.24 \pm 0.17$, $F2 = 65.70 \pm 3.44\%$ $-\Delta F/F = 1.19 \pm 0.18\%$ ($n = 5$). (B) Averaged time constants (n = 5) of the ON fluorescence for *Shaker* (○) and Shaker-IR (●) at different membrane potentials (HP = −90mV) (fit to a monoexponential function). (C) Averaged time constants ($n = 5$) of the OFF fluorescence for *Shaker* (○, ●) and Shaker-IR (■) at different membrane potentials (HP = −90mV). The OFF fluorescence was fitted to single exponential function for Sh-IR and to the sum of two exponential functions for Sh. In the presence of the inactivating "ball" a second, slower component appears in the fluorescence traces during repolarization. Note that the time constant of the fast component of Sh (○) closely follows the one of Sh-IR (■), while the second component in Sh (●) (generated by inactivated channels) is ∼10-fold slower. (D) Percentage of fast (○) and slow (●) components of the OFF fluorescence in Sh. Error bars represent SEM. When the bars are not visible, they are inside the symbols.

by the observation that, despite the prominent time-dependent decay of the ionic current, its time constant does not correlate with any components of the fluorescence kinetics. We have compared current inactivation kinetics with both ON and OFF fluorescence kinetics during 1-s depolarization in oocytes expressing the S202C mutant. These three processes were well fitted by a single exponential function and their time constants plotted against the membrane potential, as shown in Fig. 9 L. The time constants characteristic of the ionic current inactivation do not have corresponding or related time constants in the fluorescence signals but lay in between the time constants of ON and OFF fluorescence.

DISCUSSION

The intracellular regions of β_1 and β_2 subunits are responsible for most aspects of the modulation on BK_{Ca} channels (Orio et al., 2006). However, the mechanism by which β subunits exert their regulation on channel gating is still under scrutiny. To investigate the possibility that the β_2 subunit interacts directly or indirectly with BK_{Ca} main voltage sensor (S4), we have taken advantage of an optical method to directly monitor its effect on the voltage-sensing region of the channel.

As previously described for the β_2 modulation on BK_{Ca} channels (Xia et al., 1999; Wallner et al., 1999), also the cysteine mutants used in this study undergo fast inactivation when coexpressed with β_2 (Fig. 3 D). In addition, the voltage dependence of channel activation (G(V) curve) was shifted toward more negative potentials in the presence of the auxiliary subunit (Fig. 2 E, Fig. 3 C, Fig. 4 E, and Fig. 5 E). Thus, for the same membrane potential, the channel open probability is higher when the β_2 is present. Interestingly, the extent of the G(V) shift observed in this study seems smaller than the one reported for WT channels (Wallner et al., 1999; Orio and Latorre, 2005). One possible explanation is that the presence of an intact β_2 subunit (not with the N terminus deletion [IR, inactivation removed]) may be responsible for the reduced effect on the G(V) curves. Alternatively, the smaller G(V) shift could be a consequence of the R207Q mutation that by itself induces a shift of the activation curves toward more negative potentials. In agreement with this hypothesis, the mutation F315Y that increases channel open probability several times (similarly to the R207Q mutation) reduces the β_1 effect on the BK_{Ca} channel voltage sensitivity (Wang et al., 2006). Nevertheless, we found that the voltage dependence of the fluorescence changes (F(V) curves) consistently shifted on the voltage axis in the

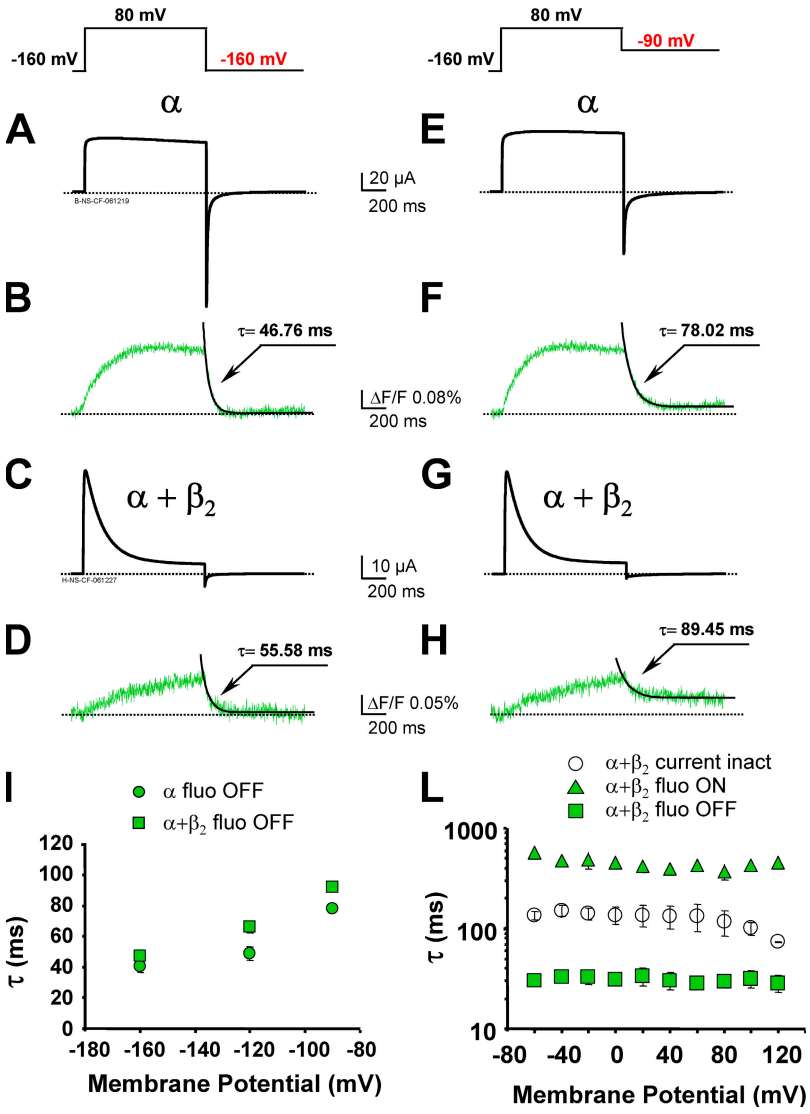

Figure 9. The β_2-induced inactivation process is not interfering with BK_{Ca} S4 segment return in the resting position. Representative K^+ current traces from oocytes expressing the α (A and E) and $\alpha+\beta_2$ subunit (S202C mutant) (C and G), elicited by 1-s depolarization from −160 to 80 mV, and repolarizations to −160 mV (A and C) and to −90 mV (E and G) (HP = −90 mV). The corresponding fluorescence traces and the best fits to a single exponential function of the OFF fluorescence are shown superimposed in B, D, F, and H. Note that the OFF fluorescence is well fitted to a single exponential function both in the presence and in the absence of β_2 subunits. (I) Time course of fluorescence return at different membrane potentials. (L) Time constants of current inactivation (○), best fitted to one exponential function from current peak to the end of the pulse (1-s pulses, as shown in Fig. 3 D), were compared with time constants of ON fluorescence (▲) and OFF fluorescence (■) (during repolarization to −160 mV) when β_2 is coexpressed, both best fitted to one exponential function. There is no correlation between the current inactivation kinetics and the fluorescence kinetics. Error bars represent SEM. When the bars are not visible, they are inside the symbols.

same direction as the G(V) curves (Fig. 3 C, Fig. 4 E, and Fig. 5 E). Since the fluorescence measurements report the voltage sensor movement (Savalli et al., 2006), our results suggest that the β_2 subunit facilitates an activated conformation of the voltage sensor. These findings are in agreement with the conclusions drawn by Bao and Cox (2005) from gating current measurements in channels formed by coexpression of the mouse BK channel (mSlo) with β_1 subunits. In that study, the Q(V) curves were shifted toward more negative potentials when β_1 was coexpressed, leading to the hypothesis that a physical interaction between the β_1 extracellular loop and the S4 can account for the stabilization of the voltage sensor in the active state. Our study, using a completely different experimental approach, suggests a similar mechanism for the β_2 subunit. The significant reduction in ΔF observed in S202C and R201C when the α and β_2 subunits are coexpressed supports the hypothesis of a close interaction between β_2 extracellular loop and the upper S4 region (Table I). In general, the extracellular loops of BK_{Ca} β subunits seem long enough to interact with the pore region, e.g., to induce rectification of the ionic current (Zeng et al., 2003) or reduce toxin accessibility to the channel outer mouth (Meera et al., 2000). We speculate that the drastic reduction in ΔF observed when β_2 is coexpressed is either due to a decreased upper S4 labeling efficiency (because of the steric hindrance of the long extracellular loop) or to a quenching effect on the fluorophores attached to residues S202C or R201C. Interestingly, the averaged ΔF of 200C labeled with TMRM was not affected by β_2 coexpression (Table I), possibly because fluorophore accessibility to this position is not reduced by the β_2 subunits. On the other hand, BK_{Ca} channel activation depends on the intrinsic closed to open equilibrium and is also allosterically coupled to voltage sensor activation and Ca^{2+} binding (Horrigan and Aldrich, 2002). Thus, it is possible that the β_2 subunit–induced facilitation of the voltage sensor activation arises from an indirect or allosteric effect.

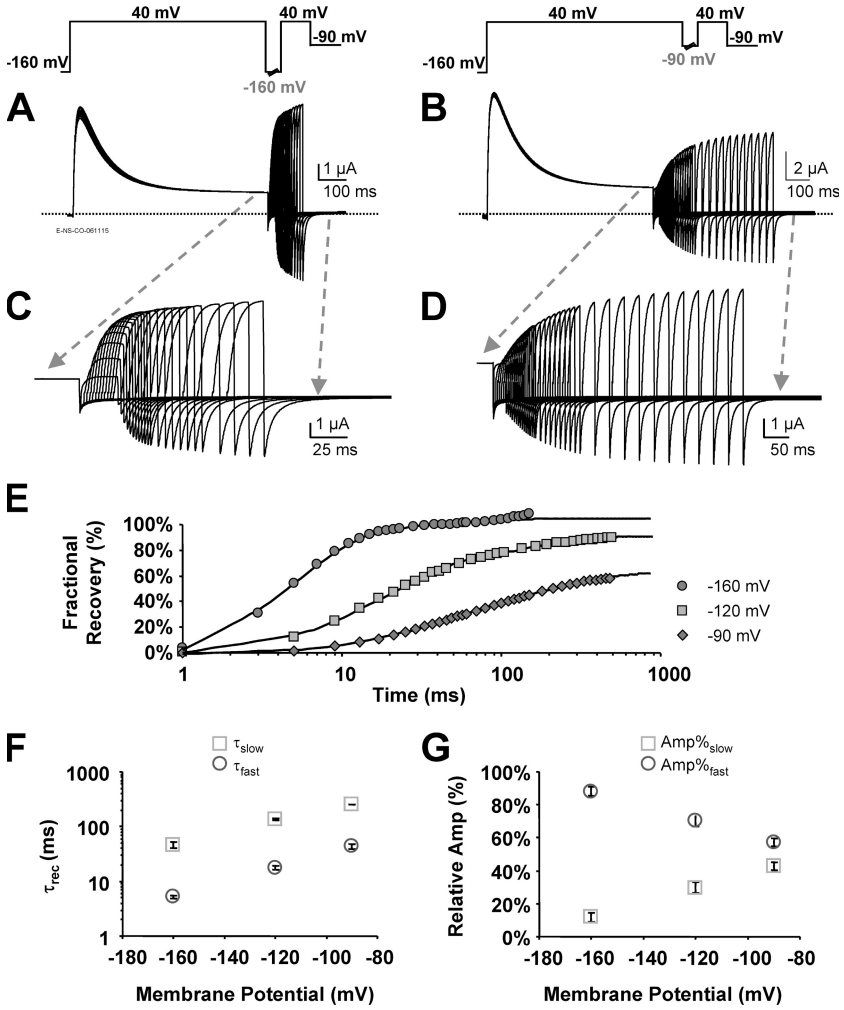

Figure 10. Voltage dependence of the recovery from β_2-induced inactivation. (A and B) Family of K^+ currents from oocytes expressing $\alpha+\beta_2$ subunits (S202C mutant) elicited by a "double pulse protocol" shown above the traces (HP = −90 mV). A 700-ms inactivating pulse from −160 to 40 mV is followed by repolarizing interpulses to −160 mV (A) or to −90 mV (B) of variable duration. A 25-ms test pulse to 40 mV is applied to monitor the recovery from inactivation. C and D are an expanded scale of the ionic current during test pulses as in A and B, respectively. (E) Semilogarithmic plot of the percentage of fractional recovery calculated as the ratio between the peak current elicited by the test pulse and the peak current elicited by the inactivating pulse for the experiment shown in A and B. The fits to biexponential functions are shown superimposed. (F) Averaged time constants for the recovery from inactivation at different membrane potentials: at −160 mV, τ_{fast} = 5.24 ± 0.35 ms and τ_{slow} = 45.87 ± 5.65 ms; at −120 mV, τ_{fast} = 17.89 ± 1.34 ms and τ_{slow} = 135.96 ± 8.27 ms; at −90 mV, τ_{fast} = 43.47 ± 3.99 ms and τ_{slow} = 248.91 ± 0.23 ms (n = 4). The relative amplitudes of the two components of the exponential fits are shown in G (at −160 mV, Amp_{fast}% = 88.23 ± 2.88% and Amp_{slow}% = 11.77 ± 2.88%; at −120 mV, Amp_{fast}% = 70.24 ± 3.25% and Amp_{slow}% = 29.76 ± 2.88%; at −90 mV, Amp_{fast}% = 57.16 ± 2.60% and Amp_{slow}% = 42.84 ± 2.88%, n = 4). Error bars represent SEM.

The coexpression with the modulatory BK_{Ca} β subunits has been also shown to have kinetic effects on current activation and deactivation (Meera et al., 1996; Brenner et al., 2000; Cox and Aldrich, 2000; Cox and Aldrich, 2000; Orio and Latorre, 2005). We have observed a slowing of current activation kinetics of the cysteine mutants when the β_2 subunit was coexpressed (Fig. 3 F, Fig. 4 F, and Fig. 5 F). The analysis of fluorescence recordings has revealed a parallel slowdown of the fluorescence onset kinetics in the presence of the β_2 subunit (Fig. 3 F, Fig. 4 F, and Fig. 5 F), suggesting that the auxiliary subunit affects the overall kinetics of the voltage-sensing region, in turn affecting the rate of current activation.

In addition to the effects on the voltage dependence and kinetics of channel activation and S4 conformational changes, the β_2 subunit also confers a fast inactivation of the ionic current to BK_{Ca} channels (Wallner et al., 1999), involving a mechanism similar to the one of N-type inactivation as in Na^+ (Armstrong and Bezanilla, 1977) and in K^+ (*Shaker*) channels (Bezanilla et al., 1991; Perozo et al., 1992; Roux et al., 1998). The immobilization of the voltage sensor is a signature of this process as the inactivating "ball," once occupying the inner pore, impedes the return of the voltage sensor to its resting position (Bezanilla et al., 1991; Perozo et al., 1992; Roux et al., 1998). We have provided the first optical evidence that the inactivating particle in the N terminus of *Shaker* channels prevents the return of the S4 segments to their resting position in the inactivated channels. This conclusion could be derived from the appearance of a second, extremely slow, new component in the OFF fluorescence kinetics, related to the N-inactivated channels (Figs. 7 and 8). Using the same experimental approach, we have probed the properties of the β_2-induced inactivation in BK_{Ca} channels to gain insight on its mechanism. We have analyzed the kinetics of the OFF fluorescence in the presence and in the absence of the β_2 subunit in the S202C mutant (Fig. 9), and we found no clear evidence of a new component in the fluorescence return during repolarization when β_2 was coexpressed, suggesting an inactivating mechanism that is not the classically described N-type inactivation. The modest decrease in the time course of the OFF fluorescence during repolarization at −160, −120, and −90 mV observed in

$\alpha+\beta_2$ compared with α alone are compatible with the previously described effect of β_2 subunits on the kinetics of BK_{Ca} activation and deactivation (Meera et al., 1996; Brenner et al., 2000; Orio and Latorre, 2005). Supporting the view that β_2-induced inactivation may not be the typical N type is also the finding that different intracellular blockers did not interfere with the inactivation process (Solaro et al., 1997), unlike that reported for *Shaker* channel (Choi et al., 1991). Although it would have been interesting to assess voltage sensor immobilization at positions other than 202, the OFF fluorescence kinetics for 200 and 201 mutants could not be reliably estimated due to the extremely small PyMPO fluorescence signal in the presence of the β_2 subunit (R201C; Fig. 5 D) and the slow relaxation and fast bleaching rate of the TMRM fluorescence signals during long depolarizations (N200C) (Savalli et al., 2006).

There are both advantages and limitations in the fluorescence-based method we used to solve the mode of operation of the β_2 subunit. Voltage clamp fluorometry has allowed us to directly track the S4 movements (for review see Tombola et al., 2006) and assess the properties of N inactivation without the use of pore blockers that could interfere with S4 movements and the inactivation mechanism. On the other hand, the hSlo BK_{Ca} channel needed to be engineered for fluorescence measurements (C-less+R207Q background). Therefore, although what we observed is consistent with previous studies, as for any mutagenesis-based study, these results should be ideally validated in the WT channel. Also, one of the assumptions of this approach is that the fluorescence reports the S4 movements, as the voltage dependence of the F(V) curve (always preceding the G(V) curve) suggests. Still, the possibility that other types of protein rearrangements can influence the fluorophore emission cannot be excluded. An alternative experimental strategy for this study could have been based on gating current measurements. However, limitations also apply to this approach; for example it requires the undesirable (as discussed above) use of K^+ channel blockers to isolate the gating current. Additionally, it is uncertain that reliable information regarding S4 movement can be extracted from BK_{Ca} channel gating currents measurements since $<50\%$ of the total charge movement is contributed by the movement of the S4 segments (Ma and Horrigan, 2005).

In summary, the shift of the F(V) curves toward more negative potential upon β_2 subunit coexpression supports the idea that the facilitation of BK_{Ca} channel activation by the β_2 subunit is a result of a change in the equilibrium of the voltage sensor. We also provide evidence that the docking of the N terminus of the β_2 subunit into the hSlo inner pore is not coupled to S4 segment immobilization. This is unlike the case of the *Shaker* channel and is consistent with the view that the BK_{Ca} channel inactivation process induced by the β_2 subunit may not follow a typical N-type inactivation mechanism.

We thank Daniel Sigg for insightful discussions.

This work was supported by National Institutes of Health (NIH)/National Institute of Neurological Disorders and Stroke RO1NS043240 and American Heart Association grant in aid 0250170N to R. Olcese, and NIH HL054970 to L. Toro.

Lawrence G. Palmer served as editor.

Submitted: 16 April 2007
Accepted: 12 June 2007

REFERENCES

Armstrong, C.M., and F. Bezanilla. 1977. Inactivation of the sodium channel. II. Gating current experiments. *J. Gen. Physiol.* 70:567–590.

Bao, L., and D.H. Cox. 2005. Gating and ionic currents reveal how the BKCa channel's Ca^{2+} sensitivity is enhanced by its β1 subunit. *J. Gen. Physiol.* 126:393–412.

Behrens, R., A. Nolting, F. Reimann, M. Schwarz, R. Waldschutz, and O. Pongs. 2000. hKCNMB3 and hKCNMB4, cloning and characterization of two members of the large-conductance calcium-activated potassium channel β subunit family. *FEBS Lett.* 474:99–106.

Bentrop, D., M. Beyermann, R. Wissmann, and B. Fakler. 2001. NMR structure of the "ball-and-chain" domain of KCNMB2, the β2-subunit of large conductance Ca^{2+}- and voltage-activated potassium channels. *J. Biol. Chem.* 276:42116–42121.

Bezanilla, F., and C.M. Armstrong. 1977. Inactivation of the sodium channel. I. Sodium current experiments. *J. Gen. Physiol.* 70:549–566.

Bezanilla, F., E. Perozo, D.M. Papazian, and E. Stefani. 1991. Molecular basis of gating charge immobilization in Shaker potassium channels. *Science.* 254:679–683.

Brenner, R., T.J. Jegla, A. Wickenden, Y. Liu, and R.W. Aldrich. 2000. Cloning and functional characterization of novel large conductance calcium-activated potassium channel β subunits, hKCNMB3 and hKCNMB4. *J. Biol. Chem.* 275:6453–6461.

Cha, A., and F. Bezanilla. 1997. Characterizing voltage-dependent conformational changes in the Shaker K^+ channel with fluorescence. *Neuron.* 19:1127–1140.

Cha, A., and F. Bezanilla. 1998. Structural implications of fluorescence quenching in the Shaker K^+ channel. *J. Gen. Physiol.* 112:391–408.

Choi, K.L., R.W. Aldrich, and G. Yellen. 1991. Tetraethylammonium blockade distinguishes two inactivation mechanisms in voltage-activated K^+ channels. *Proc. Natl. Acad. Sci. USA.* 88:5092–5095.

Cox, D.H., and R.W. Aldrich. 2000. Role of the β1 subunit in large-conductance Ca^{2+}-activated K^+ channel gating energetics. Mechanisms of enhanced Ca^{2+} sensitivity. *J. Gen. Physiol.* 116:411–432.

Diaz, L., P. Meera, J. Amigo, E. Stefani, O. Alvarez, L. Toro, and R. Latorre. 1998. Role of the S4 segment in a voltage-dependent calcium-sensitive potassium (hSlo) channel. *J. Biol. Chem.* 273:32430–32436.

Gribkoff, V.K., J.E. Starrett Jr., and S.I. Dworetzky. 2001. Maxi-K potassium channels: form, function, and modulation of a class of endogenous regulators of intracellular calcium. *Neuroscientist.* 7:166–177.

Ha, T.S., M.S. Heo, and C.S. Park. 2004. Functional effects of auxiliary β4-subunit on rat large-conductance Ca^{2+}-activated K^+ channel. *Biophys. J.* 86:2871–2882.

Hanner, M., W.A. Schmalhofer, P. Munujos, H.G. Knaus, G.J. Kaczorowski, and M.L. Garcia. 1997. The β subunit of the

high-conductance calcium-activated potassium channel contributes to the high-affinity receptor for charybdotoxin. *Proc. Natl. Acad. Sci. USA.* 94:2853–2858.

Haug, T., D. Sigg, S. Ciani, L. Toro, E. Stefani, and R. Olcese. 2004. Regulation of K^+ flow by a ring of negative charges in the outer pore of BKCa channels. Part I: Aspartate 292 modulates K^+ conduction by external surface charge effect. *J. Gen. Physiol.* 124:173–184.

Ho, S.N., H.D. Hunt, R.M. Horton, J.K. Pullen, and L.R. Pease. 1989. Site-directed mutagenesis by overlap extension using the polymerase chain reaction. *Gene.* 77:51–59.

Horrigan, F.T., and R.W. Aldrich. 2002. Coupling between voltage sensor activation, Ca^{2+} binding and channel opening in large conductance (BK) potassium channels. *J. Gen. Physiol.* 120:267–305.

Hoshi, T., W.N. Zagotta, and R.W. Aldrich. 1990. Biophysical and molecular mechanisms of Shaker potassium channel inactivation. *Science.* 250:533–538.

Hoshi, T., W.N. Zagotta, and R.W. Aldrich. 1991. Two types of inactivation in Shaker K^+ channels: effects of alterations in the carboxy-terminal region. *Neuron.* 7:547–556.

Hu, S., M.Z. Labuda, M. Pandolfo, G.G. Goss, H.E. Mcdermid, and D.W. Ali. 2003. Variants of the KCNMB3 regulatory subunit of maxi BK channels affect channel inactivation. *Physiol. Genomics.* 15:191–198.

Jiang, Z., M. Wallner, P. Meera, and L. Toro. 1999. Human and rodent MaxiK channel β-subunit genes: cloning and characterization. *Genomics.* 55:57–67.

Latorre, R., and S. Baruchi. 2006. Large conductance Ca^{2+}-activated K^+ (BK) channel: activation by Ca^{2+} and voltage. *Biol. Res.* 39:385–401.

Lippiat, J.D., N.B. Standen, I.D. Harrow, S.C. Phillips, and N.W. Davies. 2003. Properties of BK(Ca) channels formed by bicistronic expression of hSloα and β1-4 subunits in HEK293 cells. *J. Membr. Biol.* 192:141–148.

Lu, R., A. Alioua, Y. Kumar, M. Eghbali, E. Stefani, and L. Toro. 2006. MaxiK channel partners: physiological impact. *J. Physiol.* 570:65–72.

Ma, Z.M., and F.T. Horrigan. 2005. Voltage-sensing residues in the S2 and S4 segments of the BK channel. *Biophys. J.* 88:100A.

Mannuzzu, L.M., M.M. Moronne, and E.Y. Isacoff. 1996. Direct physical measure of conformational rearrangement underlying potassium channel gating. *Science.* 271:213–216.

Meera, P., M. Wallner, Z. Jiang, and L. Toro. 1996. A calcium switch for the functional coupling between α (hslo) and β subunits (Kv,caβ) of maxi K channels. *FEBS Lett.* 385:127–128.

Meera, P., M. Wallner, and L. Toro. 2000. A neuronal β subunit (KCNMB4) makes the large conductance, voltage- and Ca^{2+}-activated K^+ channel resistant to charybdotoxin and iberiotoxin. *Proc. Natl. Acad. Sci. USA.* 97:5562–5567.

Moss, B.L., and K.L. Magleby. 2001. Gating and conductance properties of BK channels are modulated by the S9-S10 tail domain of the α subunit. A study of mSlo1 and mSlo3 wild-type and chimeric channels. *J. Gen. Physiol.* 118:711–734.

Nimigean, C.M., and K.L. Magleby. 1999. The β subunit increases the Ca^{2+} sensitivity of large conductance Ca^{2+}-activated potassium channels by retaining the gating in the bursting states. *J. Gen. Physiol.* 113:425–440.

Orio, P., and R. Latorre. 2005. Differential effects of β1 and β2 subunits on BK channel activity. *J. Gen. Physiol.* 125:395–411.

Orio, P., P. Rojas, G. Ferreira, and R. Latorre. 2002. New disguises for an old channel: MaxiK channel β-subunits. *News Physiol. Sci.* 17:156–161.

Orio, P., Y. Torres, P. Rojas, I. Carvacho, M.L. Garcia, L. Toro, M.A. Valverde, and R. Latorre. 2006. Structural determinants for functional coupling between the β and α subunits in the Ca^{2+}-activated K^+ (BK) channel. *J. Gen. Physiol.* 127:191–204.

Perozo, E., R. Mackinnon, F. Bezanilla, and E. Stefani. 1993. Gating currents from a nonconducting mutant reveal open-closed conformations in Shaker K^+ channels. *Neuron.* 11:353–358.

Perozo, E., D.M. Papazian, E. Stefani, and F. Bezanilla. 1992. Gating currents in Shaker K^+ channels. Implications for activation and inactivation models. *Biophys. J.* 62:160–168.

Qian, X., X. Niu, and K.L. Magleby. 2006. Intra- and intersubunit cooperativity in activation of BK channels by Ca^{2+}. *J. Gen. Physiol.* 128:389–404.

Roux, M.J., R. Olcese, L. Toro, F. Bezanilla, and E. Stefani. 1998. Fast inactivation in Shaker K^+ channels. Properties of ionic and gating currents. *J. Gen. Physiol.* 111:625–638.

Salkoff, L., A. Butler, G. Ferreira, C. Santi, and A. Wei. 2006. High-conductance potassium channels of the SLO family. *Nat. Rev. Neurosci.* 7:921–931.

Savalli, N., A. Kondratiev, L. Toro, and R. Olcese. 2006. Voltage-dependent conformational changes in human Ca^{2+}- and voltage-activated K^+ channel, revealed by voltage-clamp fluorometry. *Proc. Natl. Acad. Sci. USA.* 103:12619–12624.

Schreiber, M., and L. Salkoff. 1997. A novel calcium-sensing domain in the BK channel. *Biophys. J.* 73:1355–1363.

Shen, K.Z., A. Lagrutta, N.W. Davies, N.B. Standen, J.P. Adelman, and R.A. North. 1994. Tetraethylammonium block of Slowpoke calcium-activated potassium channels expressed in *Xenopus* oocytes-evidence for tetrameric channel formation. *Pflugers Arch..* 426:440–445.

Solaro, C.R., J.P. Ding, Z.W. Li, and C.J. Lingle. 1997. The cytosolic inactivation domains of BKi channels in rat chromaffin cells do not behave like simple, open-channel blockers. *Biophys. J.* 73:819–830.

Stefani, E., and F. Bezanilla. 1998. Cut-open oocyte voltage-clamp technique. *Methods Enzymol.* 293:300–318.

Stefani, E., M. Ottolia, F. Noceti, R. Olcese, M. Wallner, R. Latorre, and L. Toro. 1997. Voltage-controlled gating in a large conductance Ca^{2+}-sensitive K^+ channel (hslo). *Proc. Natl. Acad. Sci. USA.* 94:5427–5431.

Tombola, F., M.M. Pathak, and E.Y. Isacoff. 2006. How does voltage open an ion channel? *Annu. Rev. Cell Dev. Biol.* 22:23–52.

Toro, B., N. Cox, R.J. Wilson, E. Garrido-Sanabria, E. Stefani, L. Toro, and M.M. Zarei. 2006. KCNMB1 regulates surface expression of a voltage and Ca^{2+}-activated K^+ channel via endocytic trafficking signals. *Neuroscience.* 142:661–669.

Tseng-Crank, J., N. Godinot, T.E. Johansen, P.K. Ahring, D. Strobaek, R. Mertz, C.D. Foster, S.P. Olesen, and P.H. Reinhart. 1996. Cloning, expression, and distribution of a Ca^{2+}-activated K^+ channel β-subunit from human brain. *Proc. Natl. Acad. Sci. USA.* 93:9200–9205.

Uebele, V.N., A. Lagrutta, T. Wade, D.J. Figueroa, Y. Liu, E. McKenna, C.P. Austin, P.B. Bennett, and R. Swanson. 2000. Cloning and functional expression of two families of β subunits of the large conductance calcium-activated K^+ channel. *J. Biol. Chem.* 275:23211–23218.

Wallner, M., P. Meera, M. Ottolia, G.J. Kaczorowski, R. Latorre, M.L. Garcia, E. Stefani, and L. Toro. 1995. Characterization of and modulation by a β-subunit of a human maxi KCa channel cloned from myometrium. *Receptors Channels.* 3:185–199.

Wallner, M., P. Meera, and L. Toro. 1996. Determinant for β-subunit regulation in high-conductance voltage-activated and Ca^{2+}-sensitive K^+ channels: an additional transmembrane region at the N terminus. *Proc. Natl. Acad. Sci. USA.* 93:14922–14927.

Wallner, M., P. Meera, and L. Toro. 1999. Molecular basis of fast inactivation in voltage and Ca^{2+}-activated K^+ channels: a transmembrane β-subunit homolog. *Proc. Natl. Acad. Sci. USA.* 96:4137–4142.

Wang, B., B.S. Rothberg, and R. Brenner. 2006. Mechanism of β4 subunit modulation of BK channels. *J. Gen. Physiol.* 127:449–465.

Wang, Y.W., J.P. Ding, X.M. Xia, and C.J. Lingle. 2002. Consequences of the stoichiometry of Slo1 α and auxiliary β subunits on functional properties of large-conductance Ca^{2+}-activated K^+ channels. *J. Neurosci.* 22:1550–1561.

Wei, A., C. Solaro, C. Lingle, and L. Salkoff. 1994. Calcium sensitivity of BK-type KCa channels determined by a separable domain. *Neuron.* 13:671–681.

Weiger, T.M., M.H. Holmqvist, I.B. Levitan, F.T. Clark, S. Sprague, W.J. Huang, P. Ge, C. Wang, D. Lawson, M.E. Jurman, et al. 2000. A novel nervous system β subunit that downregulates human large conductance calcium-dependent potassium channels. *J. Neurosci.* 20:3563–3570.

Xia, X.M., J.P. Ding, and C.J. Lingle. 1999. Molecular basis for the inactivation of Ca^{2+}- and voltage-dependent BK channels in adrenal chromaffin cells and rat insulinoma tumor cells. *J. Neurosci.* 19:5255–5264.

Xia, X.M., J.P. Ding, X.H. Zeng, K.L. Duan, and C.J. Lingle. 2000. Rectification and rapid activation at low Ca^{2+} of Ca^{2+}-activated, voltage-dependent BK currents: consequences of rapid inactivation by a novel β subunit. *J. Neurosci.* 20:4890–4903.

Xia, X.M., X. Zeng, and C.J. Lingle. 2002. Multiple regulatory sites in large-conductance calcium-activated potassium channels. *Nature.* 418:880–884.

Zarei, M.M., M. Song, R.J. Wilson, N. Cox, L.V. Colom, H.G. Knaus, E. Stefani, and L. Toro. 2007. Endocytic trafficking signals in KCNMB2 regulate surface expression of a large conductance voltage and Ca^{2+}-activated K^+ channel. *Neuroscience.* 147:80–89.

Zarei, M.M., N. Zhu, A. Alioua, M. Eghbali, E. Stefani, and L. Toro. 2001. A novel MaxiK splice variant exhibits dominant-negative properties for surface expression. *J. Biol. Chem.* 276:16232–16239.

Zeng, X.H., G.R. Benzinger, X.M. Xia, and C.J. Lingle. 2007. BK channels with β3a subunits generate use-dependent slow afterhyperpolarizing currents by an inactivation-coupled mechanism. *J. Neurosci.* 27:4707–4715.

Zeng, X.H., X.M. Xia, and C.J. Lingle. 2003. Redox-sensitive extracellular gates formed by auxiliary β subunits of calcium-activated potassium channels. *Nat. Struct. Biol.* 10:448–454.

Zeng, X.H., X.M. Xia, and C.J. Lingle. 2005. Divalent cation sensitivity of BK channel activation supports the existence of three distinct binding sites. *J. Gen. Physiol.* 125:273–286.